Nitric Oxide 87 (2019) 23–30

Contents lists available at ScienceDirect

Nitric Oxide

journal homepage: www.elsevier.com/locate/yniox

Nitration of hIAPP promotes its toxic oligomer formation and exacerbates its toxicity towards INS-1 cells

Jie Zhao[a,1], Jinming Wu[a,1], Zhen Yang[a,b], Lei Ouyang[a], Lihua Zhu[a], Zhonghong Gao[a,*], Hailing Li[a,*]

[a] Hubei Key Laboratory of Bioinorganic Chemistry & Materia Medica, School of Chemistry and Chemical Engineering, Huazhong University of Science and Technology, Wuhan, 430074, People's Republic of China
[b] Center for Bioenergetics, Houston Methodist Research Institute, Houston, TX, 77030, United States

ARTICLE INFO

Keywords:
Type 2 diabetes
hIAPP
Heme
Tyrosine nitration
Reactive oxygen species

ABSTRACT

Amyloid formation of human islet amyloid polypeptide (hIAPP) is one of the most common pathological features of type 2 diabetes (T2D). Increasing evidences have shown that the overproduction of reactive oxygen species (ROS) and reactive nitrogen species (RNS) play an important role in the development of the T2D. Interestingly, our previous studies indicated that heme could bind to hIAPP, and the complex might induce the nitration of tyrosine residue (Y37) of hIAPP in the presence of hydrogen peroxide and nitrite. However, it remains unclear about effect of the nitration on the implicated function of hIAPP in the development of T2D. In this study, fluorescent assays, transmission electron microscopy (TEM), atomic force microscope (AFM) were used to demonstrate that nitration of hIAPP significantly decreased its fibril formation. But the decreased fibril formation was not through the diminished aggregation of hIAPP monomer as suggested by the results of circular dichroism spectroscopy (CD) and gel electrophoresis assay. Surface-enhanced raman spectroscopy (SERS) indicated that nitration of hIAPP impaired the intermolecular hydrogen bonding. On the basis of these results, we hypothesize that nitration of hIAPP may block the intermolecular hydrogen bonding, leading to the inhibition of its fibril formation. In addition, cytotoxicity study of native and modified hIAPP was also performed on INS-1 cells, which revealed exacerbated toxicity of hIAPP by its nitration. The findings in this study that nitration of hIAPP promotes its oligomer formation and thus exacerbates its cytotoxicity suggests a possible link between the nitrite (or the sum of nitrite and nitrate) levels and T2D, and ameliorated nitration of hIAPP by diminishing nitrative stress might be a promising therapeutic strategy for T2D.

1. Introduction

Type 2 diabetes mellitus (T2D) is the most common chronic metabolic disorder characterized by pancreatic β-cell death that causes reduced insulin secretion [1]. Human islet amyloid polypeptide (hIAPP), also known as amylin, is a 37-amino acid peptide that is co-produced and co-secreted with insulin by the pancreatic β-cells. It has the propensity to aggregate and form amyloid fibril deposits, which are found in islet beta cells of up to 90% of patients with T2D [2]. As one of the most amyloidogenic proteins, the process of amyloid fibril formation is associated with reduced β-cell mass [3]. Interestingly, oligomeric intermediates produced during the initial process of fibril formation are believed to be the most toxic species, which may involve in oxidative stress and membrane destabilization [4–7]. Meanwhile, it has been noted that body iron stores strongly relate to the risk of T2D, and the prevalence of T2D in patients with thalassemia, a disease with high plasma heme contents, is 6–14% [8,9]. Hence, it is interesting to know the implication of heme and hIAPP in the development of T2D.

Heme is a strong pro-oxidant, and free heme participates in the generation of reactive oxygen species such as hydroxyl radicals and thus leads to increased oxidative stress [10]. Interestingly, Mukherjee et al. reported that heme could bind to hIAPP; Arg11 and His18 residues of hIAPP played important roles in the binding of hIAPP to heme [11]. Our recent studies also showed that the binding of heme inhibited the aggregation of hIAPP [12]. These findings suggested an implicated role of the binding of hIAPP to heme in the development of T2D.

Protein tyrosine nitration (PTN) is a stable post-translational modification occurring under the action of a nitrating agent by adding a

* Corresponding authors.
E-mail addresses: zhgao144@mail.hust.edu.cn (Z. Gao), lihailing86@hust.edu.cn (H. Li).
[1] Contributed equally to this work.

https://doi.org/10.1016/j.niox.2019.02.010
Received 19 September 2018; Received in revised form 27 February 2019; Accepted 28 February 2019
Available online 05 March 2019
1089-8603/

nitro group on the 3-position of the phenolic ring of the tyrosine residues [13]. PTN alters the physicochemical properties of the modified tyrosine residue and confers the change to the local chemical environment of the protein, resulting in alteration of protein function and protein-protein interactions [14–16]. Increasing evidences have shown that reactive oxygen species (ROS) and reactive nitrogen species (RNS) play central roles in β-cell death in the development of T2D [17,18]. Several studies indicated that levels of the circulating metabolites of nitric oxide were associated with T2D. Studies by Binh et al. and Zahedi et al. demonstrated that nitrite concentrations were significantly elevated in serum of T2D patients compared with controls [19,20]. Moreover, it has been reported that nitrotyrosine was found in the plasma of all diabetic patients, whereas it was not detectable in the plasma of healthy control subjects [21]. It also suggested the possible role of tyrosine nitration in the development of T2D [21,22]. It is known that heme is capable to catalyze tyrosine nitration in the presence of hydrogen peroxide and nitrite. Previous researches have demonstrated that heme could easily bind to hIAPP [11,12]. Given the presence of tyrosine residue, Y37, in hIAPP, we speculated that the binding of heme to hIAPP might subject the Y37 to the heme-induced nitration in the presence of hydrogen peroxide and nitrite. Interestingly, we previously found that nitration of Aβ, a peptide which is associated with Alzheimer's disease (AD), could inhibit its aggregation and reduce its toxicity [23,24]. It also revealed that nitration of Aβ might be an important protective mechanism for its physiological function. Worth noting is that AD and T2D have similar etiology and pathogenic features [18,25]. With these findings it suggested the implication of tyrosine nitration to the functional alteration of hIAPP.

In this study, we investigated effects of hIAPP tyrosine nitration on its structure and function by comparing synthetic hIAPP and nitrated hIAPP (3NT-hIAPP), in which the tyrosine 37 was replaced with 3-nitrtotyrosine. Multiple biochemical assays including UV–Vis absorption, thioflavin-T(ThT), Bis-ANS fluorescence assays, transmission electron microscopy (TEM), atomic force microscope (AFM), circular dichroism spectroscopy (CD), gel electrophoresis assay and surface-enhanced raman spectroscopy (SERS) were employed to detect the influence of nitration of hIAPP on its aggregation. MTT assay was employed to detect the impact of nitration of hIAPP on its toxicity toward INS-1 cells.

2. Materials and methods

2.1. Materials

hIAPP peptide ($hIAPP_{1-37}$) and the mutated peptide 3NT-hIAPP (3NT-$hIAPP_{1-37}$) were synthesized by Chinese Peptide Company (Hangzhou, China). Peptides were RP-HPLC purified to > 95%. Ferriprotoporphyrin IX chloride (hemin, which is referred to as “heme” here), 3,3′,5,5′-Tetramethylbenzidine (TMB), thioflavin T (ThT), 4,4′-dianilino-1,1′-binaphthyl-5,5′-disulfonic acid (Bis-ANS), hexafluoroisopropanol (HFIP) and rabbit polyclonal antibody against 3-nitrotyrosine (3-NT) were purchased from Sigma-Aldrich (St. Louis, MO, USA). The cell culture medium (RPMI-1640) and fetal bovine serum (FBS) were obtained from Gibco (Carlsbad, CA, USA).

All solvents and other reagents were commercially available with the highest purity. Deionized water from a Milli-Q system (Millipore, Billerica, MA, USA) was used for solution preparation.

2.2. Preparation of monomer hIAPP and heme stock solution

hIAPP and 3NT-hIAPP were dissolved in HFIP at the concentration of 1 mg/ml. Lyophilized powder was obtained after sonication for 3 min and stored at −20 °C until further use. Before each experiment, the peptides were re-dissolved in Milli-Q water and immediately diluted to the desired concentration with 5 mM phosphate buffer (PB) of pH 7.4 prior to use. The heme stock solution was made by dissolving 10 mM heme in DMSO and then aliquoted and stored in the dark at −20 °C until further use.

2.3. Dot blot immunoassay

To determine whether the tyrosine residue of hIAPP could be nitrated after binding with heme in the presence of hydrogen peroxide and nitrite, 40 μM hIAPP was incubated with 10 μM heme, 500 μM hydrogen peroxide and various concentrations of nitrite in 5 mM PB at 37 °C for 1 h. Then, 3 μL of reaction mixture was transferred to nitrocellulose membrane. The nitrated hIAPP was detected using a rabbit polyclonal antibody against 3-nitrotyrosine in this assay.

2.4. UV–Vis absorption spectroscopy

The interaction between heme and hIAPP was detected by UV–Vis absorption spectroscopy. Before the experiment, 10 μM heme was mixed with 20 μM hIAPP or 3NT-hIAPP in 5 mM PB of pH 7.4 at 37 °C for 5 min. The spectra were recorded on a UV 2550 spectrophotometer (Shimadzu Co., Japan) at room temperature with a 0.5 cm cuvette.

2.5. Peroxidase activity assay

For this experiment, TMB was employed to measure the peroxidase activity of heme-hIAPP and heme-3NT-hIAPP complexes. The reaction mixtures contained 3 mM hydrogen peroxide, 0.42 mM TMB, 1 μM heme and 2 μM peptide in 100 mM citric acid buffer of pH 5.0. The reaction was initiated by adding heme or the complex. The peroxidase activity was determined by measuring the increase in the absorbance of the resultant at 652 nm ($\varepsilon 652 = 3.9108 \times 10^4\,M^{-1}cm^{-1}$).

2.6. ThT and Bis-ANS fluorescence assay

The fibril formation of hIAPP and 3NT-hIAPP was evaluated by ThT and Bis-ANS fluorescence assay on a fluorescence spectrophotometer RF-5301(Shimadzu Co., Japan). The hIAPP and 3NT-hIAPP solutions were diluted to 16 μM in 5 mM PB (pH 7.4) and incubated at 37 °C. For fluorescence measurements, 175 μl of incubated sample was mixed with 175 μl, 32 μM ThT or Bis-ANS and shaken for 1 min prior to test. ThT fluorescence was measured with excitation wavelength at 440 nm and emission wavelength at 480 nm. Bis-ANS fluorescence was measured with excitation wavelength at 385 nm and emission wavelength at 496 nm. Excitation and emission slit widths were set at 5 nm and 5 nm, respectively.

2.7. Transmission electron microscopy

Briefly, after incubation of hIAPP (15 μM) and 3NT-hIAPP (15 μm) at 37 °C for 24 h, 30 μl of each sample was dripped on a 200-mesh Formvar-carbon coated copper grid and allowed to absorb for 10 min. The excessive solution was then removed and the grids were washed with water and air dried. Finally, the grids were stained with 5% uranyl acetate for 5 min and air dried again. Images were taken using a transmission electron microscope (HITACHI H-7000FA) with an accelerating voltage of 30 kV.

2.8. Atomic force microscopy

AFM measurements were performed under ambient conditions on a SPM 9700 instrument (Shimadzu Co., Japan) using tapping mode. The hIAPP or 3NT-hIAPP was incubated in 5 mM PB (PH 7.4) at 37 °C for 24 h. A 30 μl solution with a peptide concentration of 15 μM was deposited on freshly cleaved mica. After 10 min, the excess solution was removed and the mica was washed with deionized water and air-dried. The scanning frequency was 1 Hz. At least four regions of the mica surface were examined to ensure that similar structures existed

throughout the sample.

2.9. Surface-enhanced Raman spectroscopy

80 μM hIAPP or 3NT-hIAPP was incubated in 5 mM PB of pH 7.4 at 37 °C for 48 h. The colloidal AgNPs solution was mixed with 5 μL peptide. Then 5 μL mixture was deposited onto a quartz slide and dried at room temperature. The raman spectrum of the solid was obtained after evaporation of the solution. The SERS spectrum was obtained under the same experimental procedure and conditions used to obtain the SERS spectrum of the peptide. The excitation of the laser line was 780 nm.

2.10. Circular dichroism spectroscopy

CD spectra were recorded on a JASCO-810 (Tokyo, Japan) spectropolarimeter under a constant flow of N_2 at room temperature. A quartz cuvette with a path length of 1 mm was used. CD measurements were performed between 260 and 190 nm in a quartz cuvette with a path length of 1 mm, using a bandwidth of 1 nm, 1 s response time and scan speed of 100 nm/min. The CD samples were prepared by incubating hIAPP and 3NT-hIAPP (15 μM) in 5 mM PB of pH 7.4. Each spectrum represents an average of three accumulated scans. The relevant baseline was subtracted by running PB alone as a blank.

2.11. Gel electrophoresis analysis

hIAPP or 3NT-hIAPP (50 μM) were incubated in 5 mM PB (pH 7.4) at 37 for 0, 3, 6 and 24 h. Then they were mixed with loading buffer and separated by 4%–12% NuPAGE using MES running buffer and visualized by silver staining.

2.12. Cell culture

INS-1 rat insulinoma cells were cultured in RPMI-1640 medium supplemented with 10% FBS, 50 μM mercaptoethanol, 4 mM L-glutamine, 100 U/ml penicillin and 100 μg/ml streptomycin at 37 °C in a humidified atmosphere with 5% CO_2. And cells were grown to reach confluence of 75% prior to further experiments.

2.13. MTT assay

Cell viability was determined by MTT assay, which measured the ability of metabolically active cells to form a formazan through cleavage of the tetrazolium ring of MTT. The cells were seeded in 24-well plate at a density of 2.5×10^5 and cultured for 24 h in a humidified atmosphere at 37 °C. Then, the cells were incubated with 15 μM hIAPP or mutant for 24 h. After incubation, cells were treated with MTT solution for 4 h. The medium was aspirated and replaced with 200 μl/well of DMSO to dissolve the formazan salt. Absorbance values of formazan were determined at 570 nm with a microplate reader. Results were normalized with the control.

2.14. Data analysis

All experiments were carried out at least in triplicate. Results were expressed as mean ± SEM. The student's *t*-test was used for statistical analyses, and comparison with $p < 0.05$ was considered significant difference.

3. Results

3.1. Nitration of hIAPP

Nitration of hIAPP was examined in the heme catalytic system with hydrogen peroxide and nitrite. As shown in Fig. 1, nitration of hIAPP was observed when heme, hydrogen peroxide and nitrite were all present. And the degree of nitration was positively correlated with the concentration of nitrite. It confirms the speculation that nitration of hIAPP could be induced in the heme-associated nitration environment.

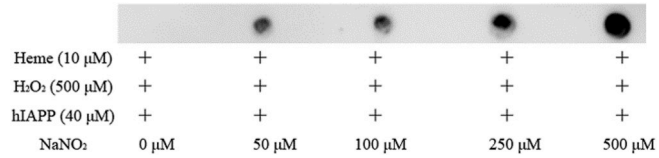

Fig. 1. Nitration of hIAPP in the heme-catalyzed nitration environment. Samples were incubated in different systems at 37 °C for 1 h. Then 3 μL of sample was transferred to nitrocellulose membranes. A rabbit polyclonal antibody against 3-nitrotyrosine was employed to detect the nitrated peptide.

3.2. Effect of nitration of hIAPP on its binding to heme and the peroxidase activity of heme-hIAPP complex

It has been reported that hIAPP could bind to heme and change the UV–Vis absorption of heme [11,12]. Thus, UV–Vis spectrometry was applied to investigate the effect of nitration of hIAPP on the interactions between heme and hIAPP. As shown in Fig. 2A, a moderate increase in the Soret band along with red shift of the peak from 385 nm to 398 nm was observed in the heme-hIAPP complex as compared to heme. Similar change was also visualized in the spectrum of heme-3NT-hIAPP. It indicates that tyrosine nitration does not alter the interaction of hIAPP with heme.

For the peroxidase activity assay, TMB was used as catalytic oxidation substrate. As shown in Fig. 2B and C, the binding of hIAPP increased the peroxidase activity of the heme, which is consistent with previous reports. Similarly, the increase was also observed in the heme-3NT-hIAPP complex. It suggests no effect of hIAPP nitration on peroxidase activity of the heme-hIAPP complex.

3.3. Fluorescent study of effect of hIAPP tyrosine nitration on its aggregation

To explore the effect of hIAPP nitration on its aggregation, ThT and Bis-ANS were used for quantitative detection of the amyloid fibrils. They are two widely used probes for the visualization and quantification of amyloid fibrillation induced by protein misfolding and aggregation [26,27]. As shown in Fig. 3A, ThT fluorescence was significantly increased after 2 h incubation with hIAPP, and the increase reached to plateau after 4 h. As a comparison, the increased fluorescent of the 3NT-hIAPP group was much lower that of hIAPP, which indicated lower degree of aggregation in 3NT-hIAPP. As a further confirmation, similar results were also found in the Bis-ANS assay that significant increased fluorescence intensity was observed upon incubating Bis-ANS with hIAPP (Fig. 3B), while the increased intensity was less potent in the group of 3NT-hIAPP. The consistent results of ThT and Bis-ANS assays suggest that aggregation of hIAPP was ameliorated by its nitration.

3.4. Morphological study of the effect of hIAPP tyrosine nitration on its aggregation

Furthermore, TEM and AFM were used to investigate the morphological change of hIAPP upon its tyrosine nitration. Fig. 4A showed a representative TEM image of native hIAPP with numerous long and cross-linked mature amyloid fibrils (Fig. 4A). On the contrary, less long and cross-linked mature amyloid fibrils were observed in the image of 3NT-hIAPP (Fig. 4B). This result indicates that nitration of hIAPP can inhibit its amyloid fibril formation.

Similarly, long and cross-linked mature amyloid fibrils in hIAPP group was also observed in the morphological image examined by AFM, while less degree of aggregates were revealed in the group of 3NT-

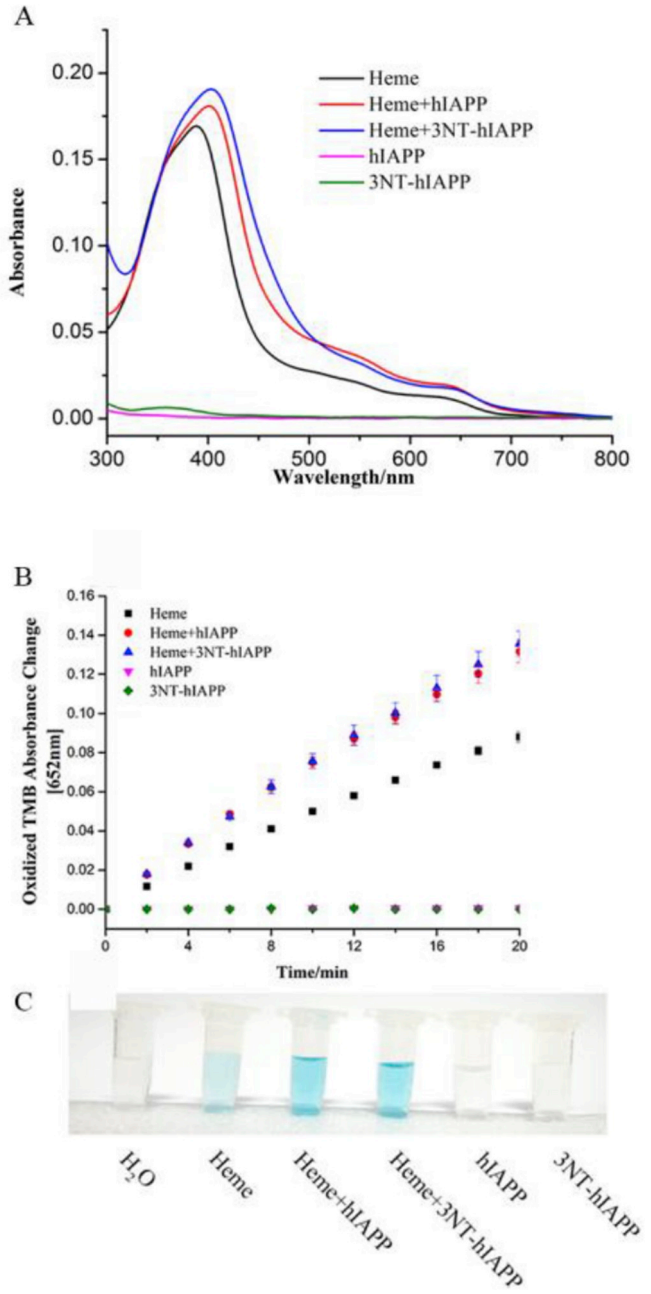

Fig. 2. Effect of nitration of hIAPP on its binding to heme and the peroxidase activity of heme-hIAPP complex. (A) UV–Vis spectra of heme-peptide complexes. 10 μM heme was mixed with 20 μM hIAPP or 3NT-hIAPP in 5 mM PB (pH 7.4) at 37 °C for 5 min before tested. Absorption spectra were recorded at equal interval after the peptides had been mixed with heme using PB as a control. (B) The specific value of the peroxidase activity of heme-peptide changes over time. The values were the absorption subtracted from that at 0 min and were presented as the mean ± SEM of three independent experiments. (C) The appearance of samples after incubation of the complex for 20 min.

hIAPP (Fig. 4C and D). The results support the notion of the fluorescence assay that nitration of hIAPP reduces its fibril formation.

3.5. CD spectroscopic analysis of effect of hIAPP tyrosine nitration on its aggregation

It is known that aggregation of proteins into amyloid fibrils is accompanied by a conformational change from α-helical to β-sheet, for which far-UV CD is an ideal approach to probe. As shown in Fig. 5A, The CD spectrum of hIAPP showed a negative peak at about 202 nm, which corresponded to random coil. After 70 min of incubation, the peak at 202 nm was decreased, meanwhile, a new peak corresponding to β-sheet at about 220 nm appeared. The change in the secondary structure of hIAPP indicates the onset of its aggregation. Similarly, a conformational change from random coil to β-sheet was also observed in the CD spectrum of 3NT-hIAPP. But the time of the appearance of the peak at 220 nm that corresponded to β-sheet was decayed to 130 min (Fig. 5B). The observation suggested that nitration of hIAPP only decreased the rate of hIAPP aggregates formation, however, the hIAPP aggregates would still form at a prolonged time of incubation even with the nitration.

3.6. SERS spectra of hIAPP and 3NT-hIAPP

It is well known that the β-sheet lamella of two adjacent peptides is primarily stabilized by the intermolecular hydrogen bonding [28]. Several researches have reported that short peptides derived from hIAPP could inhibit hIAPP aggregation by blocking the intermolecular hydrogen bonding [28,29]. We speculated that nitration of tyrosine residue of hIAPP could block the intermolecular hydrogen bonding among the peptides, and thus led to the inhibitive effect on its aggregation. In this experiment, SERS was utilized to confirm the hypothesis. Fig. 6 showed the SERS spectra of hIAPP and 3NT-hIAPP, and the detailed interpretation of the peaks were summarized in Table 1. As to hIAPP, the bands at 1334 cm^{-1} and 1447 cm^{-1} were observed, corresponding to the C—H bending mode vibration of the peptides [30–35]. As to 3NT-hIAPP, a dramatic increase was observed in the peaks of C—H bending vibration, which indicated the lack of hydrogen bonding within the peptides. In addition, a sharp peak of amide III at ~1243 cm^{-1} was appeared in the 3NT-hIAPP, suggesting the formation of a hydrated β-sheet [38] or a PPII helical structure on the surface [37–39]. Moreover, intensity of the amide band exhibited higher of the 3NT-hIAPP than that of the hIAPP, which demonstrated more disordered surface of 3NT-hIAPP than hIAPP. The increased C—H vibrations of 3NT-hIAPP also indicates the lack of hydrogen bond within the peptide. It is well known that the β-sheet lamella of two adjacent peptides is primarily stabilized by the intermolecular hydrogen bond, thus the result suggests that tyrosine nitration can decrease the stabilization of β-sheet lamella of two adjacent peptides. The result supports the diminished intermolecular hydrogen bonding by the tyrosine nitration, which leads to the inhibition effect on the hIAPP aggregation.

3.7. Gel electrophoresis analysis of the effect of hIAPP tyrosine nitration on its aggregation

Furthermore, the effect of hIAPP tyrosine nitration on its aggregation was also studied by gel electrophoresis analysis. The samples incubated at 37 °C for different times were separated by NuPAGE and followed by silver staining. As shown in Fig. 7, with the prolonged incubation time from 0 h to 24 h, molecular weight at about 3.4 kDa, which attributed to monomeric hIAPP, was correspondingly decreased in both hIAPP and 3NT-hIAPP. It suggests the occurrence of the aggregation of hIAPP and 3NT-hIAPP. At 3 h time point, the amount of unaggregated 3NT-hIAPP is a little more than the native hIAPP. When incubated for 6 h, the amount of unaggregated peptides are almost no difference between these two peptides. These results indicated that nitration of hIAPP can only partially inhibit its aggregation within 3 h, and the inhibit reaches to equilibrium after 6 h.

3.8. Effect of hIAPP tyrosine nitration on its cytotoxicity

To examine the effect of nitration of hIAPP on its toxicity, we incubated hIAPP and 3NT-hIAPP with INS-1 cells for 24 h. Then the cell viability was assessed by MTT assay. As shown in Fig. 8A, hIAPP

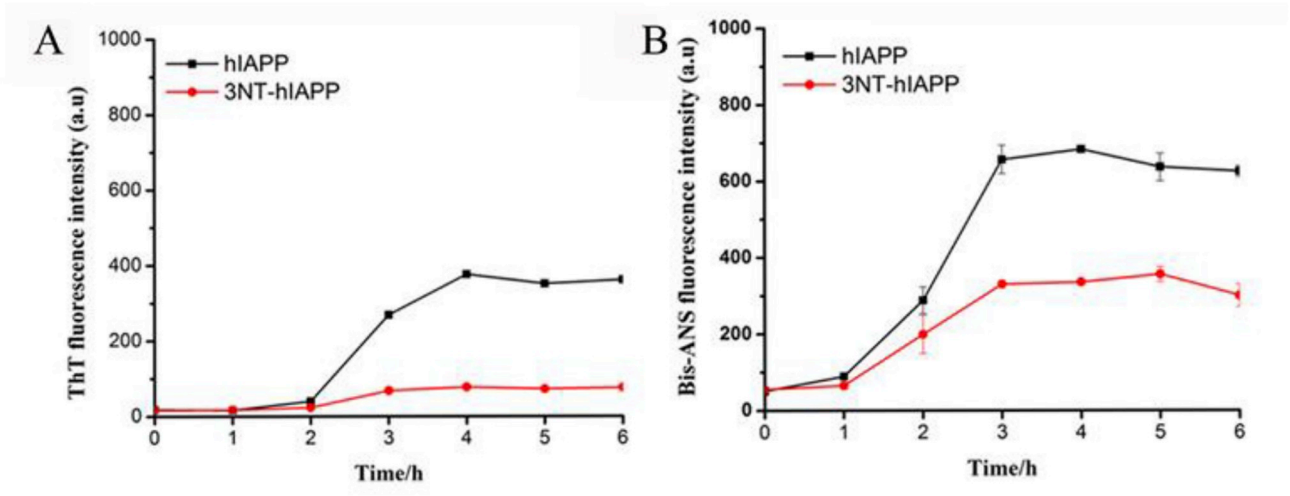

Fig. 3. ThT and Bis-ANS monitored kinetic process of aggregation for hIAPP and 3NT-hIAPP. Each sample contained 8 μM peptide, 16 μM ThT or Bis-ANS. The system was incubated at 37 °C in 5 mM PB (pH 7.4) for time intervals at 0, 1, 2, 3, 4, 5 and 6 h. The values are the mean ± SEM of triplicate experiments.

revealed strong toxicity to INS-1 cells. With dosage of hIAPP increased from 7.5 μM to 15 μM, cell viability was dropped from 54 ± 3.9% to 34.5 ± 2.4%. This result is consistent with previous reports [42]. Interestingly, 3NT-hIAPP exhibited stronger toxicity to INS-1 cells than wild types (30.3 ± 4.5% for 15 μM and 42.8 ± 3% for 7.5 μM). This result indicates that nitration of hIAPP exacerbated its toxicity toward INS-1 cells. In addition, cell morphology of each group was also examined using an inverted phase contrast microscope. As shown in Fig. 8B, the observations of each group are consistent with the results of MTT assay. The cells of the control group grew in monolayer on the culture surface with substantial lamellipodia. In contrast, after incubation with hIAPP or 3NT-hIAPP, remarkable changes in morphology occurred in INS-1 cells, which had less lamellipodia and tended to aggregate and stack. In addition, we also found that the toxicity of hIAPP or 3NT-hIAPP was dose dependent toward INS-1 cells. To further detect the mechanisms of the cytotoxicity induced by 3NT-hIAPP, HEK 293 cells were employed to determine whether the cytotoxicity of 3NT-hIAPP is specific for beta islet cells. As shown in Fig. S1, we found that there was no significant difference between the cytotoxicity of hIAPP and 3NT-hIAPP toward HEK 293 cells. It indicates that the exacerbated cytotoxicity of 3NT-hIAPP for beta islet cells may be specific.

4. Discussion

Soluble hIAPP is a 37-residue peptide synthesized in the pancreas. It is co-secreted with insulin [1] and plays an important role in regulating blood glucose with insulin [2]. Accumulation of hIAPP aggregates has been attributed to one of the main causes of β-cell failure in T2D [3]. In amyloid diseases, it is the small early forming oligomers of misfolded proteins associated with high cytotoxicity rather than the larger mature

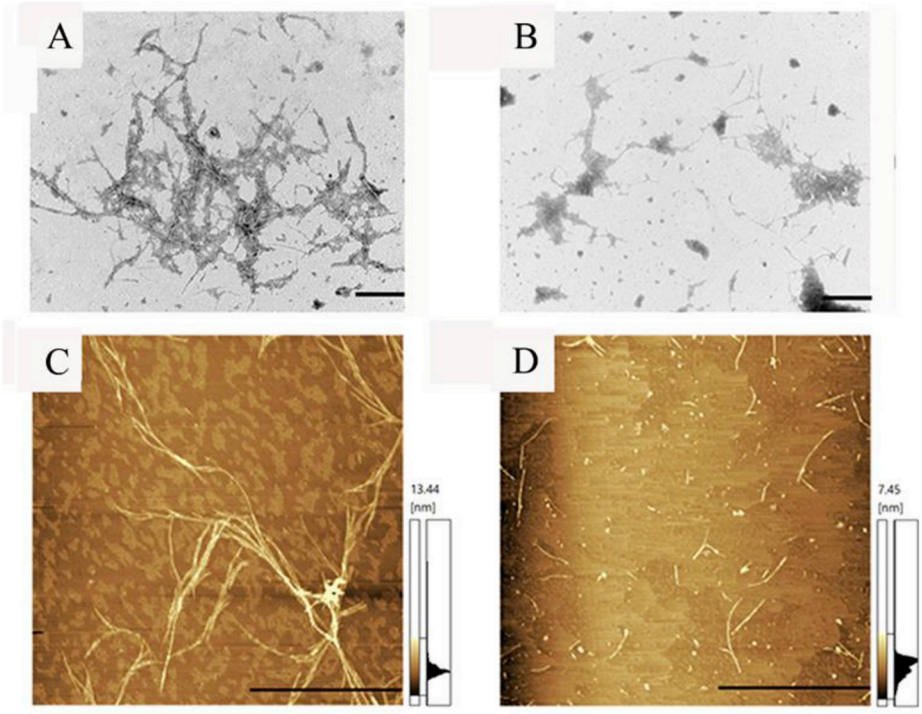

Fig. 4. Negative-stained TEM (A–B) and AFM (C–D) images of 15 μM peptide after 24 h incubation in 5 mM PB (pH 7.4) at 37 °C. (A, C) hIAPP, (B, D) 3NT-hIAPP.

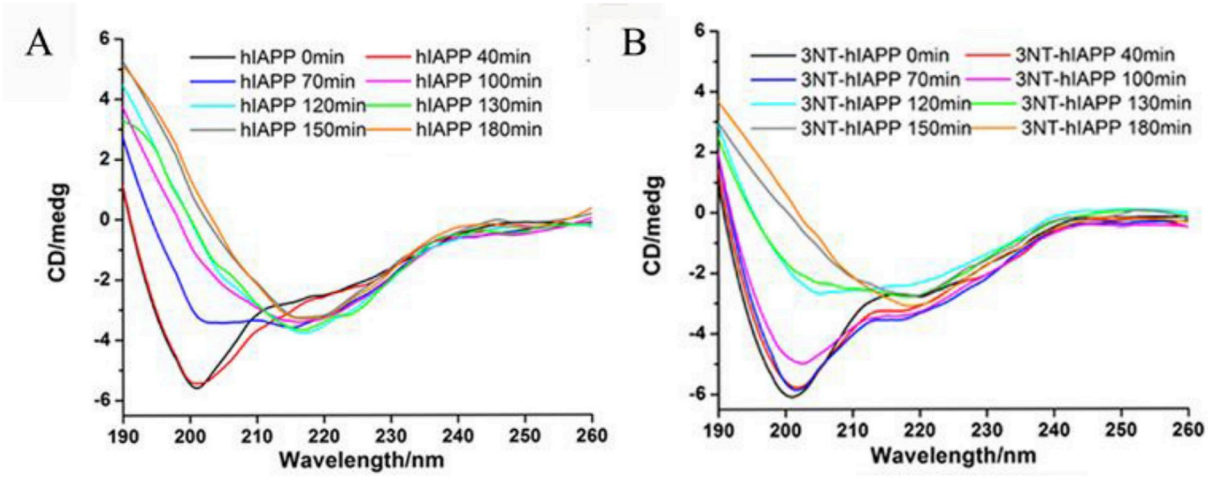

Fig. 5. CD spectra of hIAPP (A) and 3NT-hIAPP (B) at various time points.

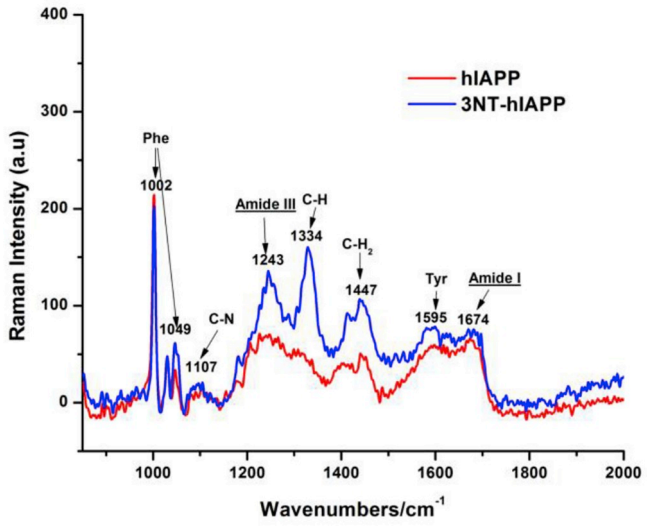

Fig. 6. SERS spectra of hIAPP and 3NT-hIAPP. 5 μL peptide (80 μM) was incubated with the nanostructured silver.

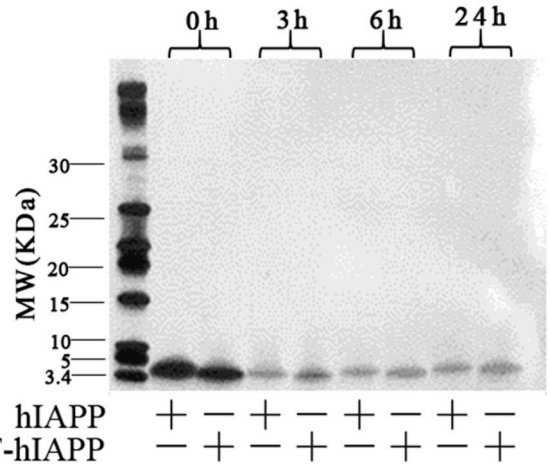

Fig. 7. Oligomerization studied by gel electrophoresis assay. 50 μM hIAPP or 3NT-hIAPP was incubated 5 mM PB (pH 7.4) at different time. Samples were separated by 4%–12% Nu-PAGE, followed by silver staining.

Table 1
Vibrational peak positions and corresponding band assignments for the recorded SERS spectra.

Raman shift (cm^{-1})	assignment	reference
1674	Amide I	[40]
1595	Tyr	[41]
1447	CH2 deformation	[30–35]
1334	CH deformation	[30-35,40]
1243	Amide III	[36–39]
1107	C–N strecth	[30,41]
1049,1102	Phe	[36, 40,41]

amyloid fibers [4–7]. As to hIAPP oligomers in T2D, however, no consensus has been reached yet. Increasing evidences have shown that mitochondrial dysfunction and oxidative stress play roles in the development of T2D [42,43]. Under oxidative stress condition, heme peroxidase activity is significantly enhanced, which increases the possibility of tyrosine nitration in hIAPP. Worth noting is that the increase of tyrosine nitration in pancreas is a prominent feature of T2D [44], suggesting that hIAPP nitration may associate with the development of the T2D.

It is important to note that there is only one tyrosine residue in the tail position of hIAPP. Although the region of 20–29 in hIAPP is generally considered as the core region for β-sheet formation, a growing number of reports have demonstrated that tyrosine 37 in hIAPP plays an important role in its aggregation [45–47]. It has been reported that hIAPP rapidly associated into transient low-order oligomers such as dimers and trimers through interaction between H18 and Y37, which suggested that Y37 was crucial for on-pathway oligomer formation [46]. Our previous study reported that Y10 in Aβ could be nitrated *in vitro* in the presence of heme, hydrogen peroxide and nitrite [23,24], and the nitration of Aβ significantly reduced its aggregation. Note that Aβ and hIAPP exhibit many common structural and physiological features, thus, we speculated that the nitration of hIAPP may have similar impact on its physiological function.

In this work, we firstly validated the nitration of hIAPP by the heme−H_2O_2−$NO_2^{\cdot}$ system (Fig. 1). The result indicated that tyrosine residue in hIAPP was the first target to be nitrated after the binding to heme in the presence of hydrogen peroxide and nitrite. Moreover, the nitration degree of tyrosine was exacerbated with the increasing level of nitrite. The results of UV–Vis spectroscopy revealed that nitration of hIAPP seemed little influence on the interaction between hIAPP and heme (Fig. 2A). Similarly, little impact of the nitration was observed on the peroxidase activity of heme-hIAPP complex (Fig. 2B and C). However, both ThT and Bis-ANS data indicated that nitration of hIAPP significantly decreased its aggregation. ThT is believed to bind to the

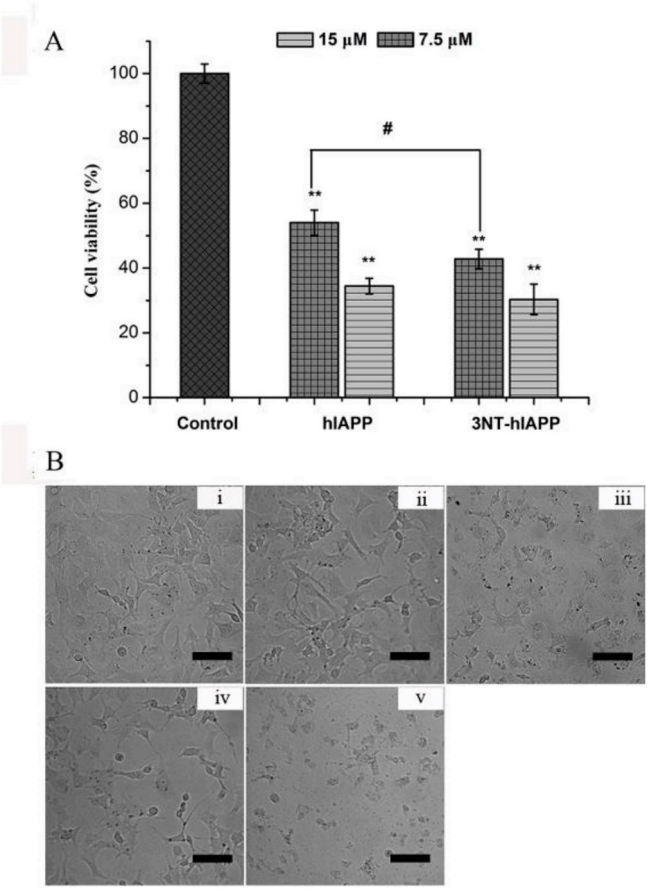

Fig. 8. Effect of hIAPP and 3NT-hIAPP on cell viability and cell morphology. (A) Cytotoxicity of hIAPP and 3NT-hIAPP to INS-1 rat insulinoma cells. The cells were treated with 15 μM and 7.5 μM aggregated hIAPP or 3NT-hIAPP for 48 h before MTT assay. Cell viability was determined using the MTT assay and was shown as a percentage of the untreated cells. Cell viability represents the mean ± SEM (n = 3). (B) Representative photomicrographs of SH-SY5Y cells incubated with different peptides for 48 h are shown: (i) control; (ii) hIAPP (7.5 μM); (iii) hIAPP (15 μM); (iv) 3NT-hIAPP (7.5 μM); (v) 3NT-hIAPP (15 μM).

grooves along the surface of the amyloid fiber, created by the repeating arrangement of side chains on the surface of the cross-β structure whereas Bis-ANS specifically binds to solvent-exposed hydrophobic surfaces of the fibrils [48–51]. They are two different mechanisms for quantifying the fibrils. Nevertheless, lower fluorescent intensity was observed in both the assays at the group of 3NT-hIAPP, which demonstrated the inhibition effect of tyrosine nitration on fibril formation. TEM and AFM confirmed the notion that the nitration dramatically inhibited the fibril formation of the hIAPP (Fig. 4B and D). On another hand, observation in the gel electrophoresis showed that 3NT-hIAPP exhibited similar potent decrease of its monomer as the native hIAPP. As noted that the fibril formation was suppressed in the nitrated hIAPP, the decreased monomer of 3NT-hIAPP was possibly attributed to the intermediate oligomer formation. The proposition was indirectly supported by the observation in the CD spectroscopic study of the conformational change of hIAPP upon the nitration. It showed that the nitration did not completely stopped the conformational change from random coil to β-sheet structure, but instead, it delayed the change rate. In a prolonged time of incubation, the conformational change from monomer to oligomers was still observed. These results suggested that nitration of hIAPP conferred its fibril formation to more reactive oligomers. It is known that the oligomers were presumed as the main toxic specie and the causative agent underlying the pathological mechanism of T2D [4–7]. Correspondingly, a more cytotoxic feature of 3NT-hIAPP

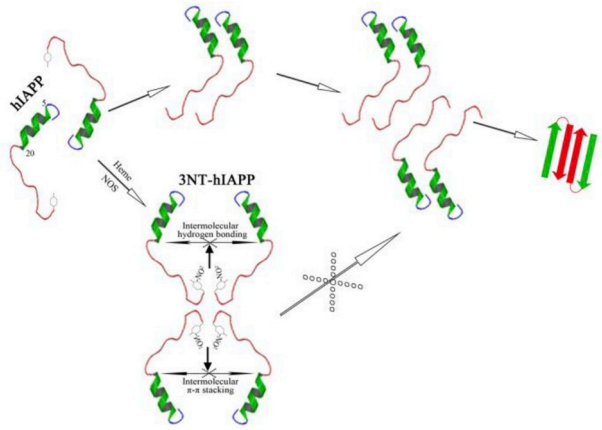

Fig. 9. Proposed mechanism of the effect of tyrosine nitration on hIAPP aggregation. hIAPP is nitrated by heme in the presence of peroxide and nitrite. Nitration of hIAPP remarkably decreases its fibril formation by blocking the intermolecular hydrogen bonding and preventing the π-π stacking interactions within the peptides. The nitrated hIAPP promotes toxic hIAPP oligomers formation and ultimately enhances hIAPP cytotoxicity *in vitro*.

was revealed in the *in vitro* cell assay as compared to the native hIAPP (Fig. 8).

Furthermore, mechanism underlying the inhibitive effect of protein nitration to hIAPP aggregation was also explored. As reported, short peptide fragments derived from hIAPP were found to inhibit hIAPP fibril formation by blocking the interaction of intermolecular hydrogen bound [28,29]. Rijkers et al. reported that introduction of N-alkylated amino acids in hIAPP broke the hydrogen bonding among the peptides and thus destabilized the β-sheet structures, which consequently inhibited hIAPP fibril formation [29]. Taken together, we speculated that nitration of tyrosine might block the intermolecular hydrogen bound to inhibit the fibril formation. SERS is a method to give information about C—H bending mode and signify the structural homogeneity in peptides [31]. The increased C—H vibrations of 3NT-hIAPP revealed in the SERS spectrum indicated the lack of hydrogen bonding within the peptides (Fig. 6). It is well known that the β-sheet lamella of two adjacent peptides is primarily stabilized by the intermolecular hydrogen bonding, thus the result suggests that tyrosine nitration can decrease the stabilization of β-sheet lamella of two adjacent peptides. In addition, the increased amide band III intensities also demonstrated that 3NT-hIAPP was more disordered than hIAPP on the surface. Furthermore, our previous work found that tyrosine nitration of Aβ significantly inhibited its aggregation, and hypothesized tyrosine nitration may decrease the interaction of the interaction of Aβ by preventing the π-π stacking interactions[23,24]. Considering the important role of Y37 for regulation of initial oligomer formation via interaction H18 in hIAPP [46], we speculated that tyrosine nitration may also affect the self-assembly processes of hIAPP through forming π-π stacking interaction, by which tyrosine nitration inhibited this interaction and decreased the fibril formation of hIAPP. This hypothesis was partially proved by CD results that the time of the appearance of peak at 220 nm that corresponds to β-sheet was decayed from 70 min to 130 min (Fig. 5). Based on the results, we proposed the mechanism that tyrosine nitration inhibited hIAPP fibril formation by blocking the hydrogen bonding and deterring the formation of π-π stacking interactions within the peptides.

In conclusion, this is the first report about the effect of hIAPP nitration on its fibril formation. Our results provide a reasonable explanation to the fact that increased heme and nitrite (or its oxidized form nitrate) levels will increase the onset of T2D: the tyrosine residue undergo nitration and forms 3NT-hIAPP in the heme and ROS catalytic environment; the nitration of hIAPP conferred the formation of fibril from its monomer to more toxic oligomers (Fig. 9). In addition, the

study suggests that attention should be drawn on the level of nitrated hIAPP in the T2D patients, and 3NT-hIAPP might be a hallmark for clinical management of T2D patients.

Acknowledgements

This work is supported by grants from the National Natural Science Foundation of China (No. 31770866, 31570810), Natural Science Foundation of Hubei Scientific Committee (No. 2016CFA001) and the Fundamental Research Funds for the Central Universities of China (2017KFYXJJ167). The Analytical and Testing Center of Huazhong University of Science and Technology is thanked for its help in CD analysis.

Appendix A. Supplementary data

Supplementary data to this article can be found online at https://doi.org/10.1016/j.niox.2019.02.010.

Conflicts of interest

The authors declare no conflicts of interest.

References

[1] J.W.M. Höppener, B. Ahrén, C.J.M. Lips, Islet amyloid and type 2 diabetes mellitus, N. Engl. J. Med. 343 (6) (2000) 411–419.
[2] J.W.M. Höppener, C.J.M. Lips, Role of islet amyloid in type 2 diabetes mellitus, Int. J. Biochem. Cell Biol. 38 (5) (2006) 726–736.
[3] R.L. Hull, G.T. Westermark, P. Westermark, S.E. Kahn, Islet amyloid: a critical entity in the pathogenesis of type 2 diabetes, J. Clin. Endocrinol. Metab. 89 (8) (2004) 3629–3643.
[4] T. Gurlo, S. Ryazantsev, C.-j. Huang, M.W. Yeh, H.A. Reber, O.J. Hines, T.D. O'Brien, C.G. Glabe, P.C. Butler, Evidence for proteotoxicity in beta cells in type 2 diabetes toxic islet amyloid polypeptide oligomers form intracellularly in the secretory pathway, Am. J. Pathol. 176 (2) (2010) 861–869.
[5] S. Zraika, R.L. Hull, J. Udayasankar, K. Aston-Mourney, S.L. Subramanian, R. Kisilevsky, W.A. Szarek, S.E. Kahn, Oxidative stress is induced by islet amyloid formation and time-dependently mediates amyloid-induced beta cell apoptosis, Diabetologia 52 (4) (2009) 626–635.
[6] L. Haataja, T. Gurlo, C.J. Huang, P.C. Butler, Islet amyloid in type 2 diabetes, and the toxic oligomer hypothesis, Endocr. Rev. 29 (3) (2008) 303–316.
[7] A. Masad, L. Hayes, B.J. Tabner, S. Turnbull, L.J. Cooper, N.J. Fullwood, M.J. German, F. Kametani, O.M.A. El-Agnaf, D. Allsop, Copper-mediated formation of hydrogen peroxide from the amylin peptide: a novel mechanism for degeneration of islet cells in type-2 diabetes mellitus? FEBS Lett. 581 (18) (2007) 3489–3493.
[8] Judith A. Simcox, Donald A. McClain, Iron and diabetes risk, Cell Metab. 17 (3) (2013) 329–341.
[9] X. Wang, X. Fang, F. Wang, Pleiotropic actions of iron balance in diabetes mellitus, Rev. Endocr. Metab. Disord. 16 (1) (2015) 15–23.
[10] D. Giugliano, A. Ceriello, G. Paolisso, Oxidative stress and diabetic vascular complications, Diabetes Care 19 (3) (1996) 257–267.
[11] S. Mukherjee, S.G. Dey, Heme bound amylin: spectroscopic characterization, reactivity, and relevance to type 2 diabetes, Inorg. Chem. 52 (9) (2013) 5226–5235.
[12] J. Wu, J. Zhao, Z. Yang, H. Li, Z. Gao, Strong inhibitory effect of heme on hiapp fibrillation, Chem. Res. Toxicol. 30 (9) (2017) 1711–1719.
[13] N. Abello, H.A.M. Kerstjens, D.S. Postma, R. Bischoff, Protein tyrosine nitration: selectivity, physicochemical and biological consequences, denitration, and proteomics methods for the identification of tyrosine-nitrated proteins, Proteome. Res. 8 (7) (2009) 3222–3238.
[14] P. Pacher, J.S. Beckman, L. Liaudet, Nitric oxide and peroxynitrite in health and disease, Physiol. Rev. 87 (1) (2007) 315-424.
[15] V. De Filippis, R. Frasson, A. Fontana, 3-nitrotyrosine as a spectroscopic probe for investigating protein–protein interactions, Protein Sci. 15 (5) (2006) 976–986.
[16] A.A. Zamyatnin, Protein volume in solution, Prog. Biophys. Mol. Biol. 24 (1972) 107–123.
[17] S. Lenzen, Oxidative stress: the vulnerable β-cell, Biochem. Soc. Trans. 36 (3) (2008) 343.
[18] Y.A. Lim, V. Rhein, G. Baysang, F. Meier, A. Poljak, M.J. Raftery, M. Guilhaus, L.M. Ittner, A. Eckert, J. Götz, Aβ and human amylin share a common toxicity pathway via mitochondrial dysfunction, Proteomics 10 (8) (2010) 1621–1633.
[19] P.N.T. Binh, Y. Abe, P.G. Tien, L.N.T.D. Son, T.T.M. Hanh, D.T.N. Diep, L.T.K. Qui, M. Kawano, C. Maruyama, Plasma nox concentrations in glucose intolerance and type 2 diabetes: a case-control study in a Vietnamese population, J. Atheroscler. Thromb. 18 (4) (2011) 305–311.
[20] S. Zahedi Asl, A. Ghasemi, F. Azizi, Serum nitric oxide metabolites in subjects with metabolic syndrome, Clin. Biochem. 41 (16) (2008) 1342–1347.
[21] C. He, H. Chul Choi, Z. Xie, Enhanced tyrosine nitration of prostacyclin synthase is associated with increased inflammation in atherosclerotic carotid arteries from type 2 diabetic patients, Am. J. Pathol. 176 (5) (2010) 2542–2549.
[22] A. Ceriello, F. Mercuri, L. Quagliaro, R. Assaloni, E. Motz, L. Tonutti, C. Taboga, Detection of nitrotyrosine in the diabetic plasma: evidence of oxidative stress, Diabetologia 44 (7) (2001) 834–838.
[23] J. Zhao, P. Wang, H. Li, Z. Gao, Nitration of y10 in Aβ(1-40): is it a compensatory reaction against oxidative/nitrative stress and Aβ aggregation? Chem. Res. Toxicol. 28 (3) (2015) 401–407.
[24] J. Zhao, J. Wu, Z. Yang, H. Li, Z. Gao, Nitration of tyrosine residue y10 of Aβ1–42 significantly inhibits its aggregation and cytotoxicity, Chem. Res. Toxicol. 30 (4) (2017) 1085–1092.
[25] D.A. Wiseman, D.C. Thurmond, The good and bad effects of cysteine s-nitrosylation and tyrosine nitration upon insulin exocytosis: a balancing act, Curr. Diabetes Rev. 8 (4) (2012) 303–315.
[26] T. Ban, D. Hamada, K. Hasegawa, H. Naiki, Y. Goto, Direct observation of amyloid fibril growth monitored by thioflavin t fluorescence, J. Biol. Chem. 278 (19) (2003) 16462–16465.
[27] C.G. Rosen, G. Weber, Dimer formation from 1-anilino-8-naphthalenesulfonate catalyzed by bovine serum albumin, N. Fluoresc. Mol. Except. Bindind prop. Biochem. 8 (10) (1969) 3915–3920.
[28] S. Gilead, E. Gazit, Inhibition of amyloid fibril formation by peptide analogues modified with α-aminoisobutyric acid, Angew. Chem. 43 (31) (2004) 4041–4044.
[29] D.T.S. Rijkers, J.W.M. Hoppener, G. Posthuma, C.J.M. Lips, R.M.J. Liskamp, Inhibition of amyloid fibril formation of human amylin by n-alkylated amino acid and alpha-hydroxy acid residue containing peptides, Chem. Eur J. 8 (18) (2002) 4285–4291.
[30] V.P. Drachev, M.D. Thoreson, E.N. Khaliullin, V.J. Davisson, V.M. Shalaev, Surface-enhanced Raman difference between human insulin and insulin lispro detected with adaptive nanostructures, J. Phys. Chem. B 108 (46) (2004) 18046–18052.
[31] D. Yugay, D.P. Goronzy, L.M. Kawakami, S.K. Claridge, T.B. Song, Z.B. Yan, Y.H. Xie, J. Gilles, Y. Yang, P.S. Weiss, Copper ion binding site in beta-amyloid peptide, Nano Lett. 16 (10) (2016) 6282–6289.
[32] C.Y. Ma, M.K. Rout, W.M. Chan, D.L. Phillips, Raman spectroscopic study of oat globulin conformation, J. Agric. Food Chem. 48 (5) (2000) 1542–1547.
[33] C. Camerlingo, F. d'Apuzzo, V. Grassia, L. Perillo, M. Lepore, Micro-Raman spectroscopy for monitoring changes in periodontal ligaments and gingival crevicular fluid, Sensors 14 (12) (2014) 22552–22563.
[34] D. Kurouski, R.P. Van Duyne, I.K. Lednev, Exploring the structure and formation mechanism of amyloid fibrils by Raman spectroscopy: a review, Analyst 140 (15) (2015) 4967–4980.
[35] J.C. Phillips, Thermodynamic description of beta amyloid formation using physicochemical scales and fractal bioinformatic scales, ACS Chem. Neurosci. 6 (5) (2015) 745–750.
[36] V. Shashilov, M. Xu, N. Makarava, R. Savtchenko, I.V. Baskakov, I.K. Lednev, Dissecting structure of prion amyloid fibrils by hydrogen-deuterium exchange ultraviolet Raman spectroscopy, J. Phys. Chem. B 116 (27) (2012) 7926–7930.
[37] S.A. Oladepo, K. Xiong, Z. Hong, S.A. Asher, J. Handen, I.K. Lednev, Uv resonance Raman investigations of peptide and protein structure and dynamics, Chem. Rev. 112 (5) (2012) 2604–2628.
[38] Z. Ahmed, I.A. Beta, A.V. Mikhonin, S.A. Asher, Uv – resonance Raman thermal unfolding study of trp-cage shows that it is not a simple two-state miniprotein, J. Am. Chem. Soc. 127 (31) (2005) 10943–10950.
[39] A.V. Mikhonin, N.S. Myshakina, S.V. Bykov, S.A. Asher, Uv resonance Raman determination of polyproline ii, extended 2.51-helix, and β-Sheet Ψ angle energy landscape in poly-l-lysine and poly-l-glutamic acid, J. Am. Chem. Soc. 127 (21) (2005) 7712–7720.
[40] A. Brambilla, A. Philippidis, A. Nevin, D. Comelli, G. Valentini, D. Anglos, Adapting and testing a portable Raman spectrometer for sers analysis of amino acids and small peptides, J. Mol. Struct. 1044 (2013) 121–127.
[41] C. Garrido, A.E. Aliaga, J.S. Gomez-Jeria, J.J. Carcamo, E. Clavijo, M.M. Campos-Vallette, Interaction of the c-terminal peptide from pigeon cytochrome c with silver nanoparticles. A Raman, sers and theoretical study, Vib. Spectrosc. 61 (2012) 94–98.
[42] M. Cnop, N. Welsh, J.-C. Jonas, A. Jörns, S. Lenzen, D.L. Eizirik, Mechanisms of pancreatic β-cell death in type 1 and type 2 diabetes, Diabetes 54 (2005) 97–107.
[43] A. Abedini, D.P. Raleigh, Destabilization of human iapp amyloid fibrils by proline mutations outside of the putative amyloidogenic domain: is there a critical amyloidogenic domain in human iapp? J. Mol. Biol. 355 (2) (2006) 274–281.
[44] P. Westermark, A. Andersson, G.T. Westermark, Islet amyloid polypeptide, islet amyloid, and diabetes mellitus, Physiol. Rev. 91 (3) (2011) 795–826.
[45] M.R. Nilsson, D.P. Raleigh, Analysis of amylin cleavage products provides new insights into the amyloidogenic region of human amylin, J. Mol. Biol. 294 (5) (1999) 1375–1385.
[46] L. Wei, P. Jiang, W. Xu, H. Li, H. Zhang, L. Yan, M.B. Chan-Park, X.-W. Liu, K. Tang, Y. Mu, K. Pervushin, The molecular basis of distinct aggregation pathways of islet amyloid polypeptide, J. Biol. Chem. 286 (8) (2011) 6291–6300.
[47] R. Kayed, J. Bernhagen, N. Greenfield, K. Sweimeh, H. Brunner, W. Voelter, A. Kapurniotu, Conformational transitions of islet amyloid polypeptide (IAPP) in amyloid formation in vitro, J. Mol. Biol. 287 (4) (1999) 781–796.
[48] N.D. Younan, J.H. Viles, A comparison of three fluorophores for the detection of amyloid fibers and prefibrillar oligomeric assemblies. ThT (thioflavin t); ANS (1-anilinonaphthalene-8-sulfonic acid); and bis-ANS (4,4 '-dianilino-1,1 '-binaphthyl-5,5 '-disulfonic acid), Biochemistry 54 (28) (2015) 4297–4306.
[49] M. Biancalana, K. Makabe, A. Koide, S. Koide, Molecular mechanism of thioflavin-t binding to the surface of beta-rich peptide self-assemblies, J. Biol. Chem. 385 (4) (2009) 1052–1063.
[50] M. Biancalana, S. Koide, Molecular mechanism of thioflavin-t binding to amyloid fibrils, Biochim. Biophys. Acta 1804 (7) (2010) 1405–1412.
[51] M. Lindgren, K. Sorgjerd, P. Hammarstrom, Detection and characterization of aggregates, prefibrillar amyloidogenic oligomers, and protofibrils using fluorescence spectroscopy, Biophys. J. 88 (6) (2005) 4200–4212.